THE ASTROPHYSICAL JOURNAL, 482:167–172, 1997 June 10

CONTEMPORANEOUS *IUE*, *EUVE*, AND HIGH-ENERGY OBSERVATIONS OF 3C 273

E. RAMOS[1] AND M. KAFATOS[2]
Center for Earth Observing and Space Research Institute for Computational Sciences and Informatics, George Mason University, Fairfax VA 22030

A. FRUSCIONE
Harvard-Smithsonian Center for Astrophysics, 60 Garden Street, Cambridge, MA 02138

F. C. BRUHWEILER
Department of Physics, Catholic University of America, Washington, DC 20064

I. M. MCHARDY
Department of Physics, University of Southampton, Southampton S09 5NH, England, UK

R. C. HARTMAN AND L. G. TITARCHUK[3]
NASA/Goddard Space Flight Center, Code 661, Greenbelt, MD 20771

AND

C. VON MONTIGNY
Landessternwarte Heidelberg-Königstuhl, D-69117 Heidelberg, Germany
Received 1996 August 16; accepted 1997 January 3

ABSTRACT

We present the results of our 1994 January and 1995 January observations of the quasar 3C 273 obtained with the *International Ultraviolet Explorer* (*IUE*) and the *Extreme-Ultraviolet Explorer* (*EUVE*). These observations were part of a large multiwavelength campaign to observe 3C 273 from radio through γ-rays. Our 1995 January photometric observations with the *EUVE* Lexan/B Deep Survey (DS) instrument indicate strong evidence for variability, at a 99% confidence level, during the 12 day observing period. We have utilized *ROSAT* PSPC soft X-ray power-law models to correlate with *EUVE* count rates. Besides variations in the normalization level between both observations, our EUV count rates are consistent with a simple power-law model with spectral index $\alpha \sim 1.77$ ($F_\nu \sim \nu^{-\alpha}$) that can be extrapolated from the soft X-rays to the EUV range. The active galactic nucleus 3C 273 is an important blazar to study because in our picture it reveals the presence of *both* disk and relativistic beam spectral contributions.

Subject headings: quasars: individual (3C 273) — ultraviolet: galaxies — X-rays: galaxies

1. INTRODUCTION

The nearby quasar 3C 273 ($z = 0.158$) is one of the best studied in all frequencies from radio through γ-rays. It possesses all the classical features of high-luminosity quasars: optical jet with high polarization, double radio lobes, superluminal motion, time variability at all frequencies (with different timescales), and a prominent *big blue bump* in the UV. The first detection in the X-rays was done by Bowyer et al. (1970). The first evidence for the existence of a soft X-ray/EUV excess came from *EXOSAT* observations below about 1 keV by Turner et al. (1985). The existence of this component was subsequently confirmed with *EXOSAT* low-energy (LE) and medium-energy (ME) spectra, and from the *Einstein* Imaging Proportional Counter (IPC) observations (Courvoisier et al. 1987) and other instruments (Turner et al. 1991). More recently, *ROSAT* Position Sensitive Proportional Counter (PSPC) observations below about 1 keV reported by Staubert (1992) show evidence of a soft excess above the extrapolation of the $\Gamma \sim 1.5$ hard X-ray power law ($F_E \propto E^{-\Gamma}$). The results of a study of the spectral shape of the soft component, as seen by *ROSAT* PSPC, were reported recently by Leach, McHardy, & Papadakis (1995). This study indicated a soft component (0.1–0.3 keV) with a photon index of $\Gamma \sim 2.7$ noncorrelated with a hard component (1.5–2.4 keV) with $\Gamma \sim 1.5$.

The source 3C 273 was one of the brightest quasars detected during the *Extreme-Ultraviolet Explorer* (*EUVE*) all-sky survey (Malina et al. 1994; Marshall, Fruscione, & Carone 1995). Because of the strong interstellar attenuation at EUV wavelengths, it was only detected in the shortest *EUVE* bandpass, the Lexan/Boron (58–174 Å or 0.071–0.214 keV), with a count rate of 0.050 ± 0.015 counts s^{-1} (Fruscione 1996). Since the launch of the *International Ultraviolet Explorer* (*IUE*) in 1978, 3C 273 has been studied extensively in the UV range (1200–3000 Å). Observations in the UV/EUV region are particularly important for this object since the blue bump (which would be the signature of an underlying accretion disk) is thought to peak in this spectral region.

Moreover, 3C 273 shows γ-ray emission detected by OSSE (Johnson et al. 1995), EGRET (Hartman et al. 1992), and COMPTEL (Hermsen et al. 1993) on board of the *Compton Gamma Ray Observatory* (*CGRO*). At energies greater than 100 MeV, the EGRET instrument has detected approximately 50 active galactic nuclei (AGNs), most of them, if not all, under the general class of "blazars," which includes BL Lacertae objects, optically violent variables (OVVs), quasars, and superluminal sources. Accepting the consensus that "blazars" are black hole–powered AGNs

[1] Please send preprint requests to eramos@mason.gmu.edu.
[2] Also Department of Physics and Astronomy, George Mason University, Fairfax, VA 22030.
[3] Also Center for Earth Observing and Space Research, CSI, George Mason University.

TABLE 1

SUMMARY OF *EUVE* AND SOFT X-RAY OBSERVATIONS OF 3C 273

Observing Dates (1)	Instrument[a] (2)	Count Rate (counts s^{-1}) (3)	$\pm\sigma$ (counts s^{-1}) (4)	K(100 Å)[b,c] (μJy) (5)	F_{EUV} photons cm^{-2} s^{-1} (6)	References (7)
1994 Jan 8–14.....	DSS	0.072	0.001	319.7	0.59	1
1995 Jan 3–15	DSS	0.044	0.004	195.4	0.36	1
1992 Dec 24–29.....	DSS	0.050	0.015	222.0	0.41	2
1992 Dec 25–29.....	*ROSAT*/PSPC	...	...	$253.0^{+8.9}_{-8.9}$[d]	0.47	3
1994 Jan 8–14.....	*ROSAT*/HRI	3.47	0.13	275.2[e]	...	4

[a] The wave bands are DSS (76–178 Å), *ROSAT* PSPC (0.1–0.3 keV), and HRI (0.1–2 keV).
[b] All fluxes were calculated assuming an energy index $\alpha = 1.77$ unless otherwise noted; K is the normalization constant.
[c] All estimates for the DSS are uncertain at a 20% level, mainly because of the uncertainty in N_H.
[d] From direct extrapolation from the *ROSAT* PSPC model.
[e] Assuming an energy index of 1.24.
REFERENCES.—(1) This paper; (2) Fruscione 1996; (3) Leach, McHardy, & Papadakis 1995; (4) McHardy 1996.

viewed along the axis of a relativistically beamed jet, it also follows that the accretion disks in these systems are being viewed nearly face-on. This is true whether the high-energy EGRET/COMPTEL emission actually arises in the beam or not. It is therefore important to examine the contribution to the emission from both the beam and the underlying accretion disk, and coordinated observations of the UV, EUV, and γ-rays provide an unique opportunity to do that (see, e.g., Lichti et al. 1995).

In this paper we present *IUE* and *EUVE* observations of 3C 273 that were part of a multifrequency campaign that involved radio, millimeter, optical, UV, X-ray, and γ-ray observations. The results from the analysis of the simultaneous observations are presented elsewhere (von Montigny et al. 1997). We show that the EUV flux is consistent with a simple, smooth, power-law model when the EUV data are compared with contemporaneous observations in the soft X-ray band below 1 keV.

2. *EUVE* OBSERVATIONS

2.1. *1994 January*

The quasar 3C 273 was observed with the *EUVE* Deep Survey Spectrometer (DSS) from January 8 16:09 UT to January 14 20:47 UT. The DSS is equipped with a photometer and three spectrometers that observe a target simultaneously. The source was observed for 96 orbits for a total effective exposure of 130,093 s over about 6 days. The effective exposure does not include high background times (e.g., during passage through the South Atlantic Anomaly) or times when the source crossed the detector "dead spot"[4] (e.g., during short jitters due to antenna slews). The spectroscopic data were characterized by a very low signal-to-noise ratio and were not used in the present analysis. However, the source was bright in the photometer, and we measured a count rate in the Deep Survey (DS) Lexan/B band (67–178 Å) of 0.072 ± 0.001 counts s^{-1}.

Lacking reliable direct EUV spectral information, we extrapolated the best-fit model to the *ROSAT* PSPC soft X-ray data (0.1–2.4 keV; Leach et al. 1995) to the EUV band. The X-ray data were obtained in 1992 December and therefore are not simultaneous with the *EUVE* observation; however, we used the extrapolation to the EUV range to estimate the EUV flux from the measured Lexan/B count rate.

We modeled the EUV to soft X-ray spectrum of 3C 273 with an absorbed power law of the following form:

$$f(\lambda) = K\lambda^{\alpha-1} \exp\{-[\sigma_{\text{H I}}(\lambda)N(\text{H I}) + \sigma_{\text{He I}}(\lambda)N(\text{He I}) + \sigma_{\text{He II}}(\lambda)N(\text{He II})]\} \times \text{photons cm}^{-2}\ \text{s}^{-1}\ \text{Å}^{-1}, \quad (1)$$

where K is the normalization factor, α is the energy index ($\alpha \equiv \Gamma - 1$), and the interstellar absorption is characterized by a cross section $\sigma_{\lambda x}$ and a column density N for H I, He I, and He II.

The EUV count rate in the DS Lexan/B band is

$$\text{count rate}|_{EUVE} = \int_{\lambda} f(\lambda)A_{\text{eff}}(\lambda)d\lambda, \quad (2)$$

where $A_{\text{eff}}(\lambda)$ is the effective area of the instrument (e.g., Malina et al. 1994). We define the total EUV flux F_{EUV} as follows:

$$F_{\text{EUV}} = \int_{\lambda_1}^{\lambda_2} f_\lambda d\lambda, \quad (3)$$

where $\lambda_1 = 76$ Å and $\lambda_2 = 178$ Å.

We fixed the Galactic hydrogen column density to $N_{\text{H I}} = 1.81 \times 10^{20}$ cm^{-2} (from high-resolution observations of the interstellar emission lines of Ti II and Ca II and the 21 cm line of H I; see Albert et al. 1993) and the ratio of helium to hydrogen column densities to $N(\text{He I})/N(\text{H I}) = 0.09$ and $N(\text{He II})/N(\text{H I}) = 0.01$ (e.g., Fruscione 1996). Using the energy index $\alpha = 1.77^{+0.13}_{-0.13}$ from the *ROSAT* PSPC observations and the measured EUV count rate, we estimate an EUV flux density at 100 Å of $K(100\ \text{Å}) = 319$ μJy from equations (1) and (2) and a total EUV flux of 0.59 photons cm^{-2} s^{-1}. If we simply extrapolate the *ROSAT* PSPC model (using the PSPC normalization at 1 keV $= f_E(1\ \text{keV}) = 0.95^{+0.22}_{-0.19}$ photons cm^{-2} s^{-1} keV^{-1}), then the estimated EUV flux density is $F(100\ \text{Å}) = 253.0^{+8.9}_{-8.9}$ μJy, and the total EUV flux is 0.47 photons cm^{-2} s^{-1}. The two flux estimates above are consistent within the approximately 20% systematic error due to uncertainties in the N_H value and in the parameters of the model.

Simultaneously with EUV, photometric *ROSAT* HRI (0.1–2 keV) observations of 3C 273 were carried out on 1993 December 13 to 1994 January 13 (McHardy 1996). They

[4] The "dead spot" is a region of decreased sensitivity near the center of the DSS detector (Vallerga et al. 1994).

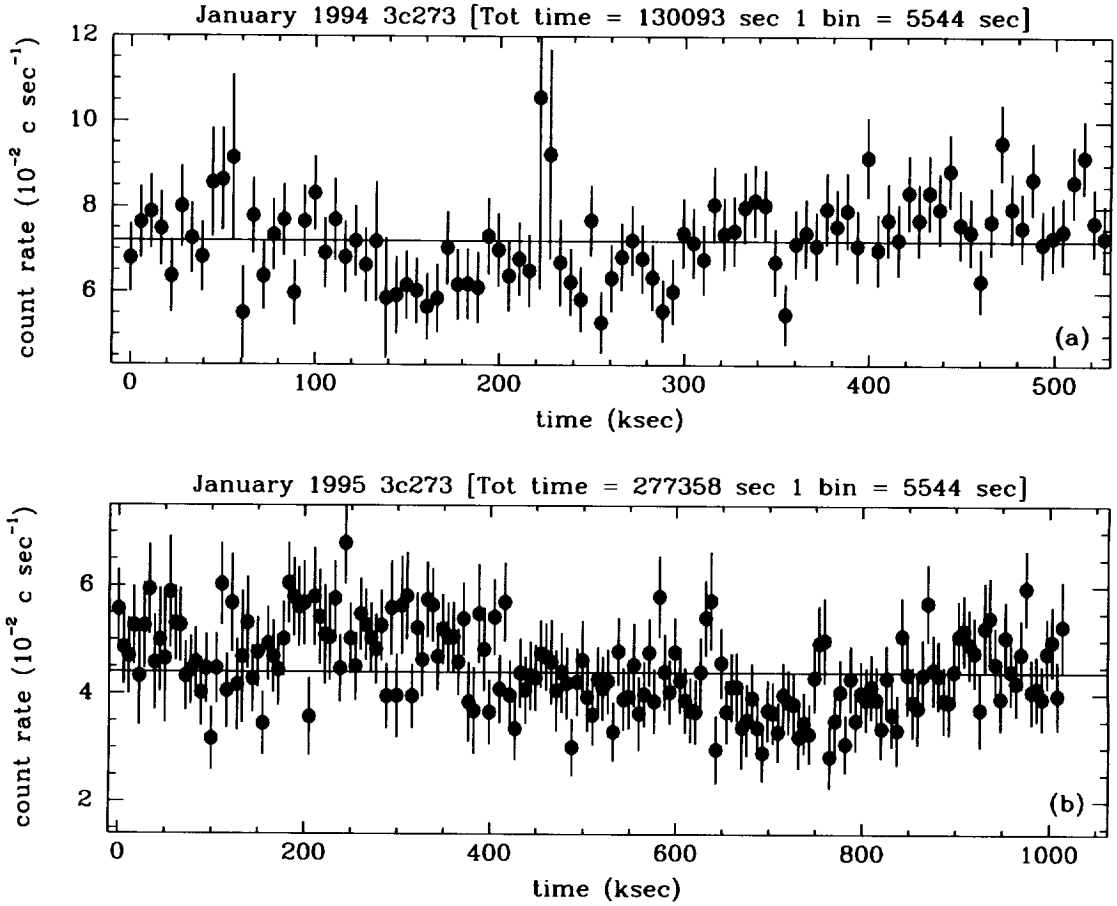

FIG. 1.—(*a*) Light curve for 1994 January *EUVE* observations with the DS Lexan/B imaging detector. The average count rate is 0.072 ± 0.001 counts s^{-1}. (*b*) Light curve for 1995 January *EUVE* observation with the DS Lexan/B imaging detector. The average count rate is 0.044 ± 0.004 counts s^{-1}.

indicate 25% variability during the 30 day observing period, with a lowest level of 3 counts s^{-1} approximately 15 days before the *EUVE* observations and a highest peak of 4 counts s^{-1} about 6 days after the *EUVE* observations.

Using the ratio between the measured *EUVE* and HRI count rates, we can constrain the EUV to X-ray spectral energy index. This calculation results in an energy index of $\alpha = 1.24^{+0.03}_{-0.04}$ and a corresponding normalization of 275.2 μJy. This flatter index may suggest the presence of a spectral break between the softer EUV/PSPC band and the harder (above 0.3 keV) HRI band. We can also perform a similar calculation using the EUV count rate obtained during the *EUVE* all-sky survey (December 25–29) 1992 and the simultaneous *ROSAT* PSPC observations. From Fruscione (1996) the observed average count rate was 0.050 ± 0.015 counts s^{-1}, which corresponds to an unabsorbed flux density of 222.0 μJy and a total EUV flux of 0.41 photons cm^{-2} s^{-1}. Our results are summarized in Table 1.

2.2. *1995 January*

Our target was observed with the *EUVE* DS instrument from 12:42 UT on 1995 January 3 to 20:04 UT January 15. The source was observed for 187 orbits, corresponding to a total effective exposure of 277,358 s. The average, error weighted count rate from 3C 273 in the Lexan/B band was 0.044 ± 0.004 counts s^{-1}. From this average count rate and the *ROSAT* PSPC spectral model presented in the previous section ($\alpha = 1.24$) we estimated the unabsorbed flux density to be 195.4 μJy at 100 Å and a total EUV flux of 0.36 photons cm^{-2} s^{-1}.

The level of the EUV emission suggests that the 1995 January observations corresponded to the baseline or "low" state of the soft X-ray /EUV variations of 3C 273, while the 1994 January observations corresponded to an "intermediate" state of 3C 273.

3. LIGHT CURVES

We extracted the light curves from photometric data using the "xtiming" package within the IRAF PROS data analysis package. To calculate the count rate, we selected a circular region around the source and an annulus for the background accurately eliminating any pixel corresponding to the "dead spot" (see § 2.1). The count rate was corrected for instrumental dead time, vignetting, and limited telemetry stream.

In order to check for possible anomalies in the light curve or errors in the corrections, we also constructed the light curve of the detector *stimpins*. These *stimpins* are electronic pulses fired at a fixed rate (1 every 4 s) to check for detector electronic stability. We binned the *stimpin* data with the same bin size as the source and applied the same corrections: the resulting corrected light curve should be constant to the 0.25 counts s^{-1} level. In the three final orbits during the 1995 January observation the correction applied to the *stimpin* did not result in the expected 0.25 counts s^{-1} count

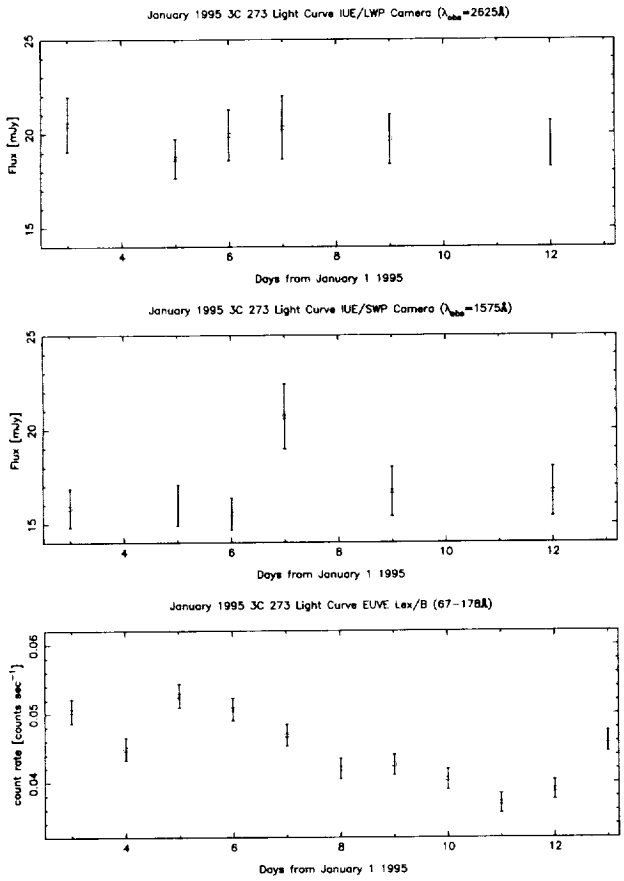

FIG. 2.—Comparison of simultaneous *IUE* and *EUVE* observations of 3C 273 for a 1 day bin during 1995 January.

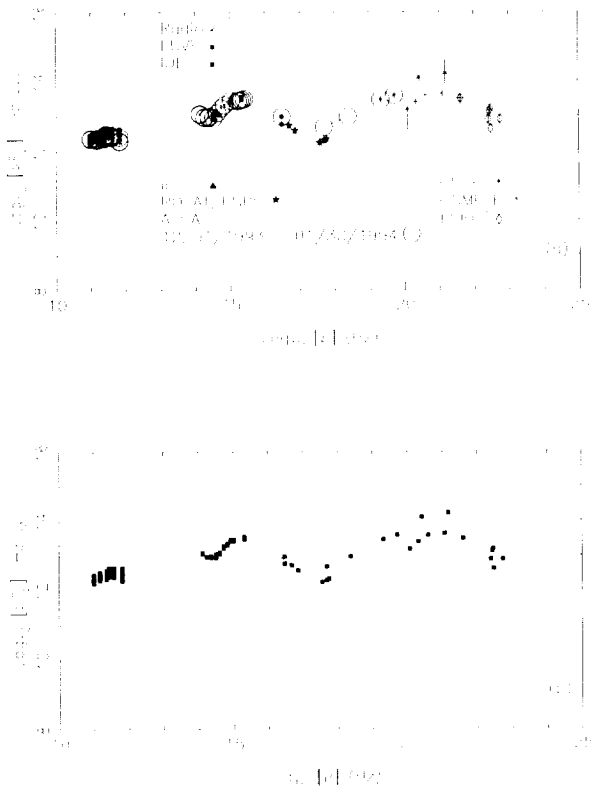

FIG. 3.—(*a*) Multifrequency spectrum of 3C 273. The soft X-ray data are taken from Leach et al. (1995); the other multifrequency data are taken from von Montigny et al. (1997). The EUV data points are from estimates presented in the paper. The open circles denote *near-contemporaneous* observations between 1993 December and 1994 January. The other data set covers the entire observing period. (*b*) Comparison of the averaged optical-UV continuum with a modified accretion disk model around a Kerr black hole (*dotted line*). The parameters of the model are as follows: mass accretion rate $\dot{M} = 1.1$, inclination angle $\cos\theta = 0.80$, and mass of the source $M = 10^9\ M_\odot$. The power-law tail [with $\alpha = 1.77^{+0.13}_{-0.13}$ and *ROSAT*/PSPC normalization $f_E(1\ \mathrm{keV}) = 0.95^{+0.22}_{-0.19}$ photons $\mathrm{cm}^{-2}\ \mathrm{s}^{-1}\ \mathrm{keV}^{-1}$] connecting the EUV to soft X-ray bands (*solid line*) is consistent with the theoretical prediction of the bulk Comptonization model discussed in the text, assuming a mean electron temperature $T_e \sim 1$–5 keV.

rate, so we eliminated these potentially problematic bins from the source analysis.

Figures 1*a* and 1*b* respectively show the corrected light curves relative to the 1994 and 1995 *EUVE* observations. The bin size is 5544 s, corresponding to one *EUVE* orbit. The effective exposure time per orbit is of the order of 1800 s since the detector operates only during the satellite daytime. We performed χ^2 tests for a constant count rate, which respectively gave $\chi^2 = 107.5$ for 96 degrees of freedom for the 1994 observations and $\chi^2 = 241.2$ for 187 degrees of freedom for the 1995 observations. For the 1994 observation the χ^2 value corresponds to a probability of 80% that the light curve is nonconstant, while for the 1995 observations it corresponds to a probability of 99%.

TABLE 2

SUMMARY OF *IUE*/SWP OBSERVATIONS OF 3C 273

Observing Dates (1)	Number of Spectra Co-added (2)	Exposure (minutes) (3)	S_ν(1200 Å) (mJy) (4)	$\pm\sigma$ (mJy) (5)
1994 Jan 8.....	2	25	13.93	0.48
1994 Jun 20	2	25	16.36	0.48
1995 Jan 3–12.....	6	25	14.46	0.36

TABLE 3

SUMMARY OF *IUE*/LWP OBSERVATIONS OF 3C 273

Observing Dates (1)	Number of Spectra Co-added (2)	Exposure (minutes) (3)	S_ν(2800 Å) (mJy) (4)	$\pm\sigma$ (mJy) (5)
1994 Jan 8.....	3	30	26.30	0.99
1994 Jun 20	3	30	27.56	0.99
1995 Jan 3–12.....	6	30	24.84	0.76

4. OTHER MULTIFREQUENCY OBSERVATIONS

The source 3C 273 was observed with the *International Ultraviolet Explorer* on 1994 January 8, on 1994 June 20, as well as from 1995 January 3–12. The 1994 January observations consisted of two exposures of 25 minutes with the SWP camera (1200–2000 Å) and three exposures of 30 minutes with the LWP camera (2000–3200 Å). The June 20 observations, with similar exposures, consisted of two pairs of observations with the SWP and LWP cameras. The 1995 January observation spanned a 9 day observation period with both SWP and LWP cameras. Since no appreciable variability was detected during the observing period, the data sets were co-added in order to increase the signal-to-noise ratio. A reddening correction for interstellar absorption of $E(B-V) = 0.03$ was applied to the extracted spectra with the reddening law of Seaton (1979). To study the continuum, the co-added spectra were binned in 50 Å intervals along the bins, which were relatively free from emission lines. In the SWP range, five bins were selected centered at $\lambda_{obs} = 1275$, 1325, 1575, 1675, and 1725 Å. In the LWP range adjacent bins were selected covering the range from 2325 to 2875 Å. For each bin a mean flux and standard deviation were computed. Our results are summarized in Tables 2 and 3 and Figures 2 and 3. In addition to the *IUE* and *EUVE* observations in Figure 3, we include contemporaneous and quasi-contemporaneous observations of 3C 273 with other instruments: *ASCA*, OSSE, COMPTEL, and EGRET (von Montigny et al. 1997).

5. DISCUSSION AND CONCLUSIONS

As pointed out, one of the most prominent observational features of 3C 273 and some other AGNs is the presence of a *big blue bump* in the infrared to UV range of the spectral energy distribution (νF_ν representation; see Fig. 3). This feature is commonly associated with thermal emission from an accretion disk around a supermassive black hole. Here we interpret the 3C 273 UV/EUV/soft X-ray spectrum in similar fashion to galactic black hole candidates as a Comptonized disk spectrum, on the basis of a simple yet self-consistent accretion disk model described in more detail elsewhere (Chakrabarti & Titarchuk 1995). Specifically, the accretion disk is divided into two main components: a standard, optically thick disk that extends to the outer boundary and produces the soft photons, and an optically thin sub-Keplerian halo that terminates in a standing shock close to the black hole. The postshock flow Comptonizes the soft (optical/UV) photons, produced in the standard disk, that are subsequently radiated as a hard spectrum with typical energy spectral index of about 1.5 ($F_\nu \sim \nu^{-\alpha}$) in the soft X-ray band. Direct radiation from the preshock Keplerian disk forms the soft component, while the photons reprocessed through Comptonization by the postshocked optically thin flow ($\tau \sim 1-2$) form the hard component. The standing shock front heats the disk to virial temperatures $T \geq 10^{11}$K as the gas reaches the centrifugal barrier. Thus, the flow puffs up, and this postshock region intercepts soft photons emitted by the standard Keplerian disk and Comptonizes them.

Alternatively, a puffed-up two temperature region may exist where the ions reach virial temperatures ($T \sim 10^{11}$–10^{13} K, the upper limit being applicable for Kerr black holes). This region terminates in the radius of marginal stability of the disk ($1.2r_g$ around a Kerr black hole) and an outer limit typically located at $30r_g \leq r_0 \leq 100r_g$ (where $r_g = GM/c^2$). This two-temperature disk was proposed by Shapiro, Lightman, & Eardley (1976) and Eilek & Kafatos (1983) for both Cygnus X-1 and AGNs. Such a disk produces a Comptonized soft X-ray spectrum as well, with the added benefit that relativistic pairs are formed with Lorentz factors $\gamma \geq 300$ (see below).

We compared our IR-optical-UV data [log (ν) ~ 14.5–15.3] with a variety of accretion disk models tabulated recently by Siemiginowska et al. (1995). In all the models the basic assumptions are the following: the disk radiates locally as a blackbody (where the effective temperature for each annulus is given by Shakura & Sunyaev 1973), and the structure of the disks is determined from Novikov & Thorne (1973) and Page & Thorne (1974). General relativistic effects on the propagation of light are also included, using the transfer function of Laor, Netzer, & Piran (1990). We compared our data with pure blackbody accretion disk models in the Schwarzschild and Kerr geometries and the modified versions, which include the effects of electron scattering opacities. We found that the averaged IR/optical/UV spectra can be well described with a modified accretion disk model around a Kerr black hole with a mass accretion rate $\dot{M} \sim 1.1$ (in units of $\dot{M} \equiv 4\pi M m_p/\sigma_T c$, where M, G, m_p, and σ_T are the mass of the black hole, the gravitational constant, the mass of the proton, and the Thompson cross section, respectively), inclination angle $\cos\theta = 0.80$ with respect to observer, and a black hole mass of $10^9\ M_\odot$ (see Fig. 3*b*). From this accretion rate $\dot{M}$, obtained in our IR/optical/UV observation modeling, we deduce a characteristic power law with an energy index of about 1.5–1.7 and a mean electron temperature $T_e \sim 1$–5 keV. This energy index is consistent with the hard power law (~ 1.7) observed in the EUV/soft X-ray observations of 3C 273 and interpreted as Comptonized radiation of the soft photons originating in the cool, standard disk.

Finally, we propose here that the overall spectrum of 3C 273 contains *both* contributions from an accretion disk and Comptonization of the disk spectrum, as well as radiation that arises in a beam (discernible at millimeter and γ-rays). A more complete model would include the coupling of the accretion disk to the beam. The energetic electrons of the beam (or powerful outflow) with Lorentz factors $\gamma \gg 1$ upscatter very effectively the disk soft radiation (with characteristic frequency ν_0). A broken power law with a break frequency $\gamma\nu_0$ can be produced as a result of multiple scatterings of the disk soft photons off the outflow electrons, where the break frequency occurs at energies ≥ 1 MeV, Sunyaev & Titarchuk (1980) showed that this break feature is always present in the Comptonization spectrum if the characteristic width of the injected spectrum is much less than the mean of the electron energy. In the thermal Comptonization case (Sunyaev & Titarchuk 1980), the soft photons are scattered off the Maxwellian electrons, which can move toward or away from the observer. Thus, at any scattering the photons lose or gain energy depending off which electrons they scatter. The envelope of the first, second, and n-scattered photon spectra is always a power law until the photons gain more energy than the electrons have. In the case of the relativistic outflow, the apparent gain or loss of energy by photons is a very strong function of scattering angle and the line of sight. Titarchuk & Lyubarskij (1995) demonstrated that a power law is formed even in the case of a monoenergetic electron distribution.

Thus, in the framework of the model of the bulk motion Comptonization, the two power-law indices of the broken power law occurring at a few MeV (see, e.g., McNaron-Brown et al. 1997) are related to the optical depth of the outflow gas, the Lorentz factor, and the electron distribution. Following this prescription we obtain the Lorentz factor $\gamma \sim 300$ from the observations. Such Lorentz factors are precisely predicted in the hot ion-dominated inner disks (Eilek & Kafatos 1983). In the future, we shall make detailed theoretical interpretations of the high-energy (γ-ray) component of the spectrum.

In summary, from our 1995 January photometric observations of 3C 273 with the *EUVE*/DSS instrument, we have strong indications of variability at a 99% confidence level during the 12 day observing period. Contemporaneous observations with the SWP and LWP cameras on the *IUE* indicates a possible correlation between the SWP light curves and the *EUVE*/DSS. Assuming a spectral model for the EUV/soft X-rays taken from *ROSAT* PSPC observations and from the average count rate obtained from the DSS observations, we were able to obtain an estimate of the flux density for both observation periods. From comparison with contemporaneous *ROSAT* HRI observations during 1994 January we are able to conclude that 3C 273 was at an "intermediate" level in the EUV/X-rays variations during that period and at a "low" level during the 1995 January observing period. Besides differences in the normalization levels of 3C 273, our EUV count rates appear to be consistent with a simple power-law shape that can be extrapolated from the soft X-rays to the EUV. Our observations seem to be consistent with a bulk Comptonization model (Chakrabarti & Titarchuk 1995) that can explain very well the continuum emission from optical to soft X-rays. We further suggest that the spectrum of 3C 273 contains contributions from an accretion disk (optical/UV), Comptonization of the disk spectrum (UV/X-rays), and radiation that arises in a beam (discernible at OSSE/COMPTEL/EGRET regions). The observational presence of a spectral *break* between the soft and hard γ-rays may be due to a scenario of multiple scatterings of the accretion disk photons off the outflow relativistic electrons with $\gamma \geq 300$.

The work of E. R. and M. K. is supported by NASA grant NAG 5-2360. We would like to thank Paul Hertz, Peter Becker, John Wallin, and W. N. Johnson for helpful discussions and suggestions.

REFERENCES

Albert, C. E., Blades, J. C., Morton, D. C., Lockman, F. J., Proulx, M., & Ferrarese, L. 1993, ApJS, 88, 81
Bowyer, C. S., Lampton, M., Mack, J., & de Mendonca, F. 1970, ApJ, 161, L1
Chakrabarti, S. K., & Titarchuk, L. G. 1995, ApJ, 455, 623
Courvoisier, T. J.-L., et al. 1987, A&A, 176, 197
Eilek, J., & Kafatos, M. 1983, ApJ, 271, 804
Fruscione, A. 1996, ApJ, 459, 509
Hartman, R. C., et al. 1992, ApJ, 385, L1
Hermsen, W., et al. 1993, A&A, 97, 97
Johnson, W. N., et al. 1995, ApJ, 445, 182
Laor, A., Netzer, H., & Piran, T. 1990, MNRAS, 242, 560
Leach, C. M., McHardy, I. M., & Papadakis, I. E. 1995, MNRAS, 272, 221
Lichti, G. G., et al. 1995, A&A, 278, 711
Malina, R. F., et al. 1994, AJ, 107, 751
Marshall, H. L., Fruscione, A., & Carone, T. E. 1995, ApJ, 439, 90
McHardy, I. M. 1996, private communication
McNaron-Brown, K., et al. 1997, ApJ, 474, L85
Novikov, I. D., & Thorne, K. S. 1973, in Black Holes, ed. C. DeWitt & B. De Witt (New York: Gordon & Breach), 344
Page, D. N., & Thorne, K. S. 1974, ApJ, 191, 499
Seaton, M. J. 1979, MNRAS, 187, 73
Shakura, N. I., & Sunyaev, R. A. 1973, A&A, 24, 337
Shapiro, S. L., Lightman, A. P., & Eardley, D. M. 1976, ApJ, 204, 187
Siemiginowska, A., et al. 1995, ApJ, 454, 77
Staubert, R. 1992, in X-Ray Emission from AGN and the Cosmic X-Ray Background, ed. W. Brinkmann & J. Trümper (MPE Rep. 235), 42
Sunyaev, R. A., & Titarchuk, L. G. 1980, A&A, 86, 121
Titarchuk, L., & Lyubarskij, Y. 1995, ApJ, 450, 876
Turner, M. J. L., Courvoisier, T., Staubert, R., Molteni, D., & Trümper, J. 1985, in Proc. 18th ESLAB Symp., ed. A. Peacock (Dordrecht: Reidel), 623
Turner, T. J., Weaver, K. A., Mushotzky, R. F., Holt, S. S., & Madejski, G. M. 1991, ApJ, 381, 85
Vallerga, J. V., Eckert, M., Sirk, M., Siegmund, O., & Malina, R. F. 1994, Proc. SPIE, 2280, 57
von Montigny, C., et al. 1997, ApJ, in press